

# Investigation of ANN structure on predicting the fracture behavior of additively manufactured Ti-6Al-4V alloys

Mohsen Sarparast (✉ [mohsen.sarparast@rockets.utoledo.edu](mailto:mohsen.sarparast@rockets.utoledo.edu))

The university of Toledo <https://orcid.org/0000-0002-9159-8460>

Majid Shafaie

Amirkabir University of Technology <https://orcid.org/0000-0002-3140-5495>

Ahmad Memaran Babakan

K. N. Toosi University of Technology

Mohammad Davoodi

K. N. Toosi University of Technology

Hongyan Zhang

The university of Toledo

---

## Research Article

**Keywords:** ANN, Machine learning, Additive manufacturing, Modified GTN Fracture

**Posted Date:** January 18th, 2023



**DOI:** <https://doi.org/10.21203/rs.3.rs-2488963/v1>

**License:**   This work is licensed under a Creative Commons Attribution 4.0 International License.

[Read Full License](#)

---

# Investigation of ANN structure on predicting the fracture behavior of additively manufactured Ti-6Al-4V alloys

Mohsen Sarparast<sup>1</sup>, Majid Shafaie<sup>2</sup>, Ahmad Memaran Babakan<sup>3</sup>, Mohammad Davoodi<sup>3</sup>, and Hongyan Zhang<sup>1</sup>

## ABSTRACT

Selective laser melting (SLM) is a prevalent additive manufacturing (AM) technique for the fabrication of metallic components. A modified GTN (Gurson-Tvergaard-Needleman) model was developed, based on the understanding of the SLM process and SLM-manufactured parts, in order to characterize void growth and void shear mechanism to predict the ductile fracture behavior of SLM-fabricated Ti6Al4V alloys under uniaxial stress states. The effect of the number of hidden layers and neurons, as a basic parameter of an artificial neural network (ANN), on predicting parameter relation accuracy was investigated. In this study resulted due to the complex relation among GTN fracture parameters and fracture displacement, defining more hidden layers in ANN improves the accuracy of predicting the damage and fracture behavior of SLM-fabricated Ti6Al4V alloys under uniaxial stress states; however, forecasting maximum force is achieved accurately by fewer hidden layers in comparison with fracture displacement needing to higher layers to predict precisely. Furthermore, the system  $R^2$ -value reaches higher accuracy more than 0.99 for both maximum force and fracture displacement based on selected hidden layers and neurons.

## Keywords

ANN, Machine learning, Additive manufacturing, Modified GTN Fracture

## Introduction

Reducing design and manufacturing time is crucial in any manufacturing process, and it is more so in additive manufacturing (AM). Additive manufacturing is a powerful technique in digital-manufacturing objects from three-dimensional (3D) models by depositing materials layer by layer. Complex structures that are difficult to be produced through traditional manufacturing processes can be easily fabricated by AM processes (1-4).

---

<sup>1</sup> Department of Mechanical, Industrial & Manufacturing Engineering, The University of Toledo, Toledo, OH, USA.

<sup>2</sup> Department of Mechanical Engineering, Amirkabir University of Technology, Tehran, Iran.

<sup>3</sup> Department of Mechanical Engineering, K. N. Toosi University of Technology, Tehran, Iran.

Corresponding author: Mohsen Sarparast  
Email: Mohsen.sarparast@rockets.utoledo.edu

Among various AM processes, sintering laser melting (SLM) is common to produce metallic parts and manufacture final parts from powder. It has obtained attention from different industries, such as biomedical and aerospace. Among titanium alloys, Ti6Al4V is a common alloy for the SLM process owing to its high strength-to-weight ratio, low density, high fracture toughness, excellent corrosion resistance, and excellent biocompatibility(5-7).

Regarding AM components applications, they are under exposure to complex stress and damage therefore investigation and evaluation of their fracture behavior is a controversial topic among scientists. Many researchers investigated these components' damage and fracture behavior and obtained different results in computational modeling and experimental analysis. They developed micromechanical models of complex ductile fracture and considered micro-void nucleation, growth, and coalescence (8-11). Gurson (12) achieved a micromechanical-based model to predict material behavior initiated by spherical cavities' growth. Then, Tvergaard and Needleman (13) modified Gurson model and considered void coalescence into a constitutive model via the dependence of the yield function on the void volume fraction (GTN modified model). Alexander et al. (14) studied the fracture behavior of SLM additively manufacture Ti-6AL-4V alloy in an experimental and computational modeling investigation and observed that combined triaxiality and load angle parameters have more accuracy in contrast to no stress state-dependence.

In order to the GTN fracture model able to predict the fracture property precisely, there are some coefficients in the GTN fracture model that are necessary to be calibrated by experimental test, therefore it needs much time and equipment for trial and error. Recently, digital fabrication technology attracted more attention to optimize process parameters, address defects, and monitor quality. The artificial neural network model (ANN) is a good tool for information processing, learning, and adopting the environment to solve problems. It has a strong ability in predicting network boundaries and finding complex relations among parameters and consequently optimization of the process (15-18).

Many scientists tried to use ANN in AM process to save time and train an ANN model to optimize parameters and achieve desired machine setting of fabrication. Wang et al (19) observed ANN is a good assistant for optimizing process parameters and defect monitoring. Chinchankar et al. (20) applied ANN to predict the surface roughness of fused deposition modeling parts based on process parameters and utilized machine learning algorithms to model ANN. Their results showed the two hidden layers with 150 neurons have better prediction accuracy in comparison to one hidden layer with 250 neurons. Mehrpouya et al (21, 22) used ANN for the investigation of the effect of process

parameters on mechanical properties, density, and temperature transformation and they found a prediction model for optimization of manufacturing parameters in AM of NiTi alloy. Kowen et al (23) studied the quality of printed parts in the SLM process and utilized ANN to find laser power and its effect on crack and pore form. Also, Stathatos et al (16) applied ANN in laser-based AM process for prediction of temperature evolution and density of fabricated parts. Jimenez (24) applied ANN for analyzing the fatigue life of nodular cast iron and by synthetic data effectively increased ANN forecast as a complementary input data.

In ANN the neurons and hidden layers number as training parameters for solving the problem affect the accuracy of the prediction model(25, 26). In this study, NN was trained by different hidden layers and neurons tried to investigate the effect of the number of neurons and layers on the accuracy of forecasting of GTN fracture model parameters. Moreover, the ANN is used to predict the complex relations among input and output data in GTN fracture model of SLM-fabricated parts of Ti6Al4V alloy.

### Preparing specimen

The experimental test the Ti-6Al-4V alloy specimens were fabricated by SLM AM process According to ASTM F2924 standard (27). Fig. 1 shows the printed specimens that took place in an Argon environment for 3 hours at 650 °C for the heat treatment process.

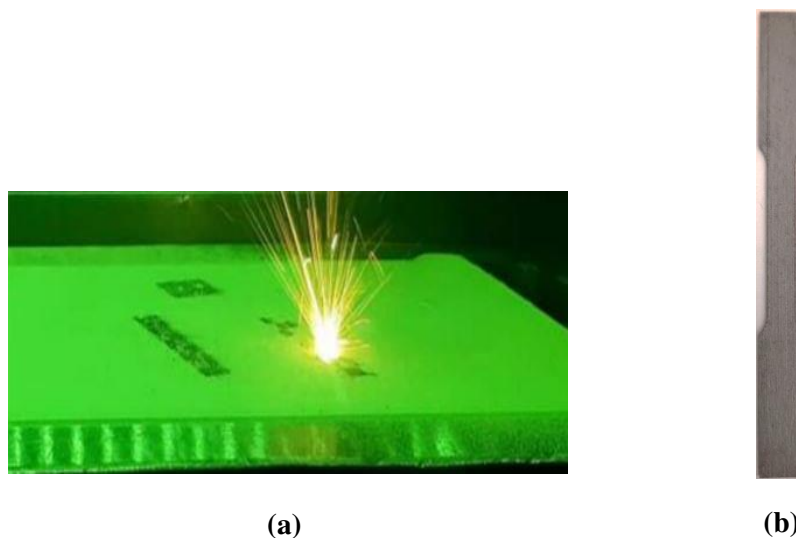


Fig 1. SLM Ti-6Al-4V alloy (a) Manufacturing process (b) Uniaxial test specimen

## Tension test

In order to analyze the mechanical behavior of SLM printed Ti-6Al-4V alloys parts, the tensile tests were conducted by the SANTAM STM150 machine test and the loading speed was at about 0.3 mm/min in tests (Fig2). Table 1 shows the mechanical property of additive-manufactured Ti-6Al-4V alloys extracted from the uniaxial tension test. The mechanical test has been conducted to extract the elastic-plastic property of the material. The Voce hardening law was considered to describe the hardening behavior of the material as follows (28):

$$\sigma_f = B - (B - A) \cdot e^{-m \cdot (\varepsilon_0 + \varepsilon^p)} \quad (1)$$

Where A, B, m, and  $\varepsilon_0$  are Voce hardening law coefficient.

Table 1. Mechanical properties of Ti-6Al-4V AM sheets.

PROPERTY	VALUE
DENSITY (KG/M <sup>3</sup> )	4800
YOUNG'S MODULUS (MPA)	105000
POISSON'S RATIO	0.342
INITIAL YIELD STRESS (MPA)	920
UTS (MPA)	987
A	985
B	-30
M	302
$\varepsilon_0$	0.009



Fig 2. Machine setup for the tensile test(29).

### Finite element simulation

In this study, FE commercial software (Abaqus) is utilized for finite element simulation and calibration of GTN fracture model (30). In this case, the Python script in Abaqus is linked with MATLAB software, and the GTN parameters were developed(31). The VUMAT subroutine is used to simulate the damage behavior of a property. Also, eight nodes with reduced integration of 3D solid elements(C3D8R) are chosen for the finite element simulation model. When damage value (D) is equal to one the element will be eliminated.

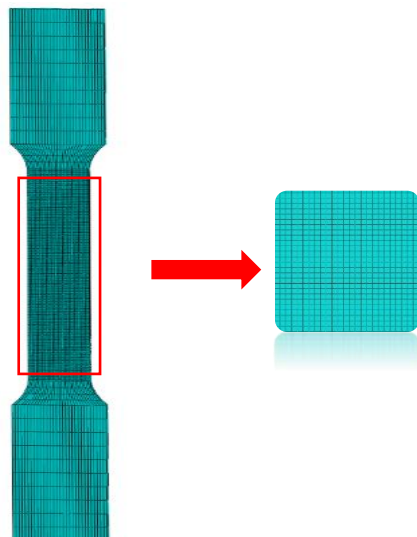


Fig 3. Finite element simulation models uniaxial test

The GTN fracture model was initially introduced by Gurson, then it was modified by Tvergaard and Needleman which is common in ductile and plasticity mechanics to define damage and fracture

behavior of metallic materials (12, 28, 32, 33). But this model is unable to consider the void shear failure in low and negative-stress triaxiality. Nahshon and Hutchinson modified GTN fracture model and imposed void coalescence, void nucleation, and shear damage as a coefficient to the model.

$$\Phi = \frac{q^2}{\sigma_y^2} + 2q_1 f^* \cosh\left(-\frac{3q_2 p}{2\sigma_y}\right) - (1 + (q_3 f^*)^2) = 0 \quad (2)$$

In Nahshon and Hutchinson's shear damage equations  $\sigma_y$  is the yield stress,  $q$  is the von mises equivalent stress,  $p$  is the hydrostatic pressure,  $f^*$  is the effective void volume fraction and  $q_1$  to  $q_3$  are constants and dependent on the material's properties:

$$f^*(f) = \begin{cases} f & f \leq f_c \\ f_c + \frac{1/q_1 - f_c}{f_f - f_c} (f - f_c) & f_c < f \end{cases} \quad (3)$$

$$\dot{f}_s = k_\omega f \omega(\boldsymbol{\sigma}_{ij}) \frac{s_{ij} \dot{\varepsilon}_{ij}^p}{q} \quad (4)$$

$$\dot{f}_g = (1 - f) \dot{\varepsilon}^p \quad (5)$$

$$\dot{f}_n = A \frac{s_{ij} \dot{\varepsilon}_{ij}^p}{q} \quad (6)$$

$$A = \begin{cases} \frac{f_N}{s_N \sqrt{2\pi}} \exp\left[-\frac{1}{2} \left(\frac{\bar{\varepsilon}_m^p - \varepsilon_N}{s_N}\right)^2\right] & P \leq 0 \\ 0 & P > 0 \end{cases} \quad (7)$$

$$\dot{f} = \dot{f}_g + \dot{f}_n + \dot{f}_s \quad (8)$$

Where  $k_\omega$  is introduced as a new material parameter for the void nucleation rate of damage in pure shear conditions, and  $\omega(\boldsymbol{\sigma})$  is the stress- function used by Nahshon and Hutchinson,  $S$  is the deviatoric stress tensor and  $\dot{\varepsilon}^p$  plastic strain rate tensor,  $f_c$  is the critical volume fraction of voids and  $f_f$  is the volume fraction of the void at the fractured moment This function is between the zero and one value, which for the axial stress state is zero and for the shear stress condition is one. Also,  $\dot{f}$  is rate of change in the voids volume fraction,  $\dot{f}_g$  is the void growth,  $\dot{f}_n$  the nucleation rate,  $\dot{f}_s$  is the shear rate of the voids.

According to table 2 the effect of nine modified GTN parameter variations on maximum force and fracture displacement by FE simulations in 36 samples used as input data for ANN modeling. The nine parameters in the constitutive equation of modified GTN are utilized in the ANN algorithm. These parameters include constitutive parameter ( $q_1, q_2$ ), initial void volume fraction ( $f_0$ ), critical void volume fraction ( $f_c$ ), void volume fraction at failure ( $f_f$ ), the void volume fraction of nucleated voids ( $f_n$ ), the standard deviation of the distribution ( $S_n$ ), and the mean value of the nucleation strain ( $E_n$ ), and shear coefficient ( $k_w$ ).

Table 2. The modified GTN parameter, maximum force, and fracture displacement data to train NN(29).

NO	Inputs									Outputs	
	q 1	q 2	f 0	f c	f f	S n	f n	E n	K w	Fmax	FD
1	1	0.75	0	0.005	0.01	0.1	0.01	0.1	0	5796.624	0.656477
2	1.5	0.75	0	0.005	0.01	0.1	0.01	0.1	0	5795.857	0.646894
3	1	1	0	0.005	0.01	0.1	0.01	0.1	0	5796.553	0.650822
4	1	0.75	0.005	0.005	0.01	0.1	0.01	0.1	0	5557.266	0.280373
5	1	0.75	0	0.005	0.25	0.1	0.01	0.1	0	5796.624	1.22118
6	1	0.75	0	0.005	0.01	0.2	0.01	0.1	0	5797.075	0.760963
7	1	0.75	0	0.005	0.01	0.1	0.1	0.1	0	5783.165	0.490098
8	1	0.75	0	0.005	0.01	0.1	0.01	0.3	0	5798.241	0.801735
9	1	0.75	0	0.005	0.01	0.1	0.01	0.1	50	5796.63	0.618433
10	1.5	1	0.005	0.1	0.25	0.2	0.1	0.3	50	5742.734	0.773149
11	1	0.812967	0.000826	0.005	0.011732	0.136897	0.1	0.1	0	5779.344	0.484892
12	1	0.917722	0.00346	0.005	0.062686	0.133368	0.068302	0.169017	44.25426	5770.09	0.501218
13	1	1	0.004626	0.005	0.043408	0.100122	0.062846	0.196965	18.63707	5759.842	0.437288
14	1	0.917722	0.00346	0.005	0.062686	0.133368	0.068302	0.169017	44.25426	5770.09	0.501218
15	1	0.971539	0.002251	0.007041	0.01	0.1	0.086423	0.142982	21.52688	5775.257	0.510772
16	1	0.894113	0.003257	0.005	0.01	0.184493	0.081619	0.183241	37.7882	5770.585	0.489313
17	1	0.934298	0.001474	0.005	0.108756	0.1	0.1	0.1	0	5773.152	0.481938
18	1	0.774382	0.005	0.005	0.068589	0.156589	0.024984	0.136766	11.32583	5725.286	0.475001
19	1	0.841393	0.00391	0.005	0.011554	0.132524	0.068759	0.182259	26.52156	5768.415	0.47945
20	1	1	0.005	0.005	0.034	0.1	0.093053	0.298693	36.46328	5745.015	0.493335
21	1	0.978156	0.004814	0.005	0.058813	0.1	0.089623	0.223808	18.22531	5749.232	0.451586
22	1	0.945697	0.005	0.005	0.01	0.143263	0.014558	0.200277	0	5572.037	0.278147
23	1	0.939513	0.004121	0.005	0.046009	0.1	0.065897	0.174042	18.85946	5767.749	0.499801
24	1	0.887675	0.00262	0.005	0.058807	0.140833	0.058419	0.18712	20.83491	5777.094	0.539225
25	1	0.901614	0.005	0.005	0.09984	0.101499	0.060116	0.155947	11.87717	5718.09	0.447309
26	1	0.950558	0.003989	0.005	0.064809	0.100246	0.053865	0.223759	8.772346	5771.276	0.58074
27	1	0.829491	0.004345	0.005	0.034783	0.135541	0.050991	0.167512	20.29329	5758.697	0.419001
28	1	0.821593	0.004653	0.005	0.066102	0.128977	0.054604	0.16716	16.80624	5735.14	0.419052
29	1	0.872989	0.004365	0.005	0.030576	0.12662	0.054683	0.22514	21.27534	5768.202	0.50447
30	1	0.861285	0.004401	0.005	0.021042	0.138414	0.037399	0.163228	17.92148	5764.118	0.441014



31	1	0.8835	0.004442	0.005	0.018634	0.138551	0.036252	0.161086	32.37898	5760.947	0.428442
32	1	0.945575	0.004152	0.005	0.034314	0.100029	0.048001	0.190853	29.14383	5769.354	0.533541
33	1	0.866755	0.004422	0.005	0.036293	0.147873	0.059633	0.172271	31.22699	5742.753	0.382974
34	1	0.932651	0.004269	0.005	0.019845	0.138969	0.059868	0.140231	18.87184	5735.889	0.366438
35	1	0.896648	0.004499	0.005	0.051262	0.134238	0.046769	0.176476	22.52134	5756.132	0.424102
36	1	0.918501	0.004384	0.005	0.026097	0.1336	0.039757	0.166472	12.12199	5763.917	0.444408

## ANN Modelling

ANN stems from a collection of artificial neurons that are trained by the environment and initial data. It is used as an effective tool for network classification with combining of numbers hidden layer neurons and training function. In this study, the ANN was trained by the Levenberg-Marquardt (34) algorithm to compute the outputs of the neurons and an activation function operates the summation of input data and weight of the neurons. Hyperbolic tangent activation function was applied to neurons of the hidden layer, and linear activation function was utilized to neurons of the output layer. The sample data was split into three sections randomly, about 70% of the samples were selected for the training of the net, 15% of samples for testing the net and the rest 15% were chosen for validation of data. Fig. 4 shows the design of the N-layer network which contains different hidden layers from 1 to 3 including variable neurons from 1 to 22 and each hidden layer is investigated individually. As mentioned before the input samples were randomly split, so the accuracy of the net and the results change when the net is trained by different data, to approach a better net to predict the phenomena in each case several different sets are trained to obtain the best net results. In other words, initially, one hidden layer with a different number of neurons is assessed then in each step by specific neurons numbers, several sets of training data is being tested and the best net results are chosen as the predicted net model, next this process is repeated for next two hidden layers include different neurons in each layer and several training sets, finally, the similar process is performed for 3 hidden layers.

The net performance and results are analyzed by calculating R-squared correlation ( $R^2$ ) parameters; therefore, the net predicts the equations more accurately whenever  $R^2$  is closer to 1. The nine GTN parameters are chosen as input parameters to predict the complex effect of this parameter on the fracture behavior of materials. Moreover, the maximum force ( $F_{max}$ ) and fracture displacement (FD) are achieved as the output parameters of ANN and are verified by experimental results.

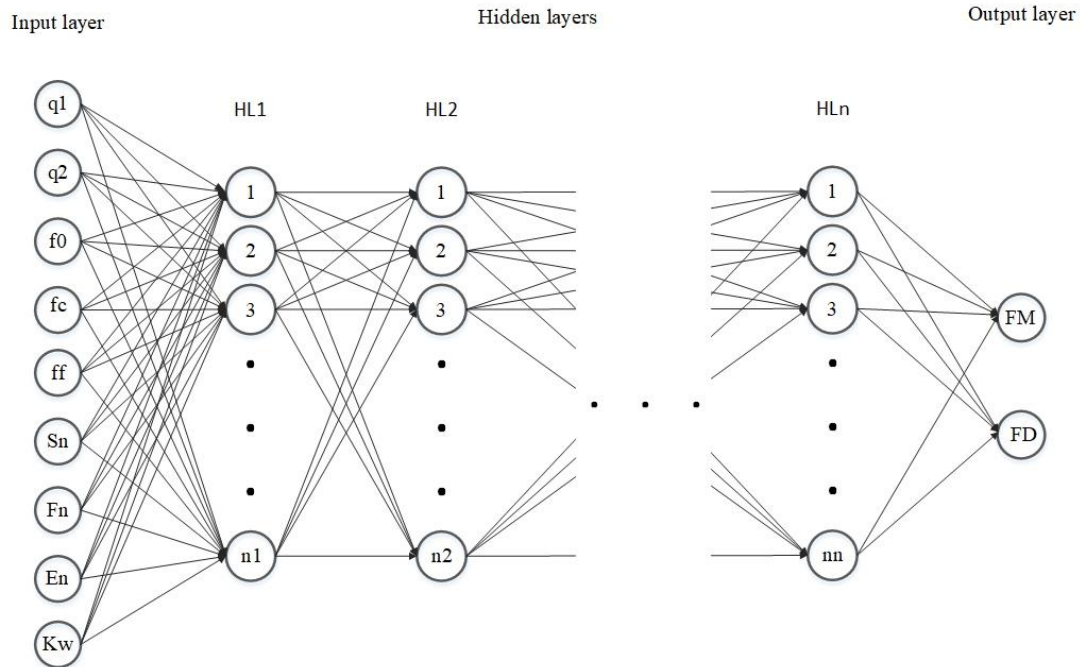
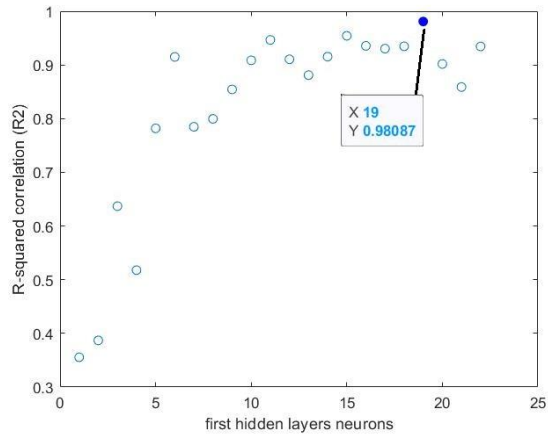


Fig. 4. Designed N-layer network

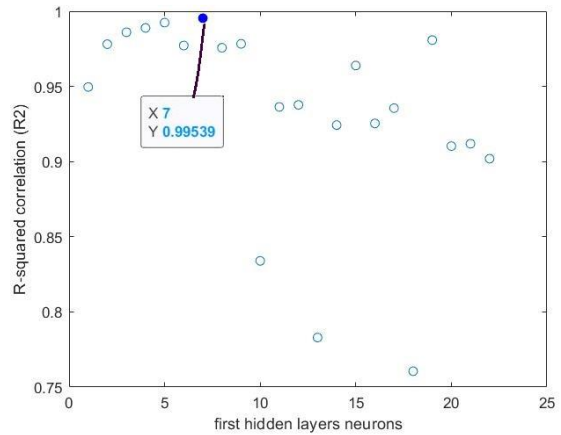
## Results and discussion

To investigate the effect of the number of neurons on the prediction accuracy of the relationship between parameters, NN is trained by three different hidden layers by the number of neurons 1 to 22 in each layer, Figs. 5, 6, and 7 show the results in each hidden layer for two output results. According to the obtained results, three hidden layers have the most suitable and accurate prediction near the experimental test. It shows that fewer neurons are enough for maximum force and there are simple relations among parameters to predict the best results.

Although adding a hidden layer causes better accuracy of predicted results, it cannot result from such a conclusion for the number of the hidden layer; because the maximum force needs fewer neurons to predict the results.



(a)



(b)

Fig 5. (a) Fracture displacement (b) Maximum force one layer

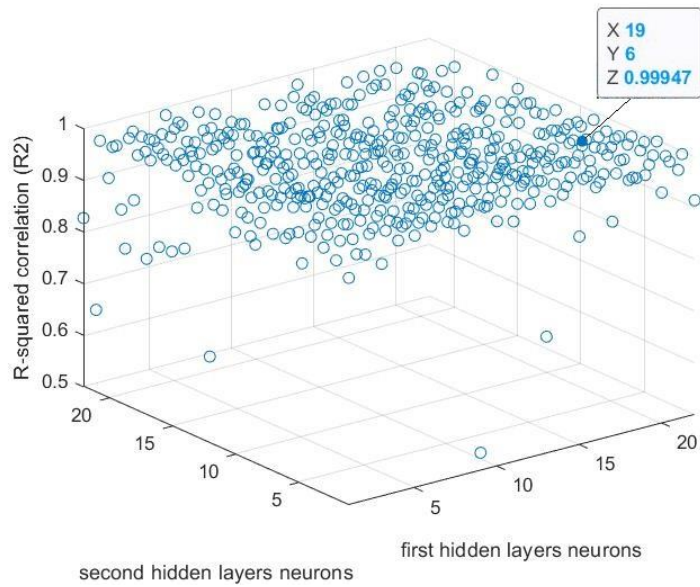


Fig 6. Maximum force two-layers

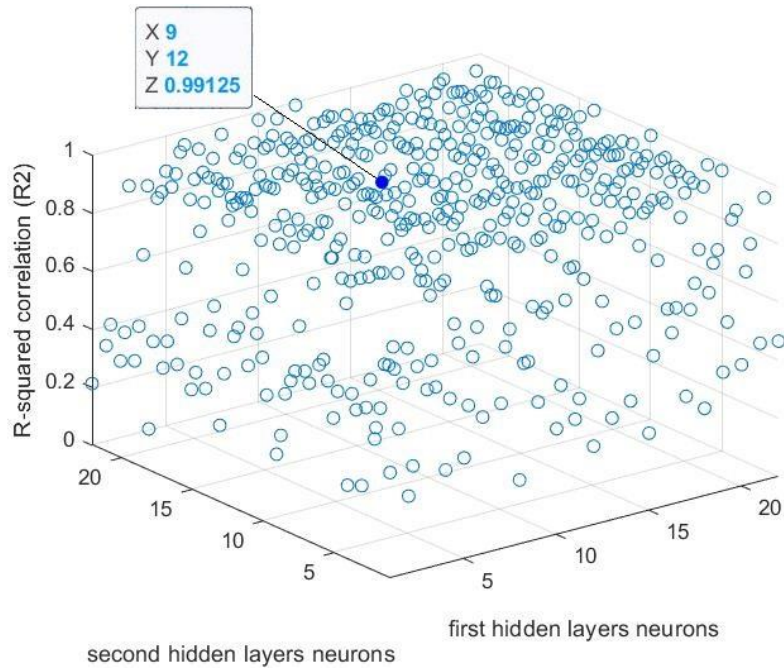


Fig 7. Fracture displacement two-layers

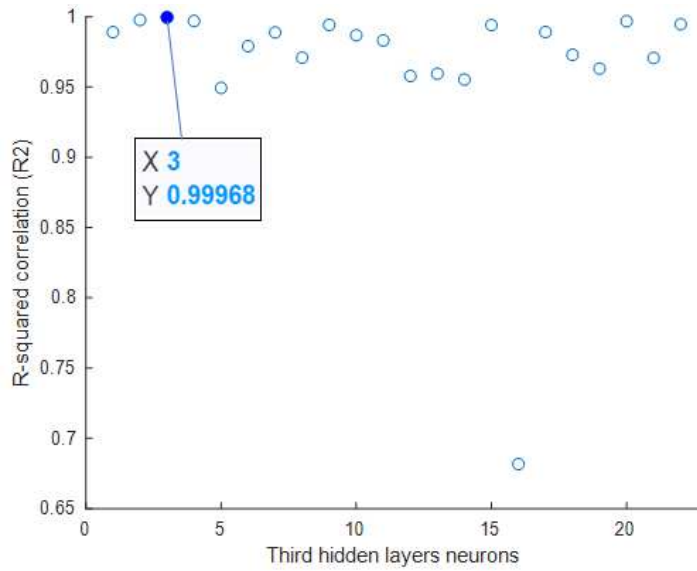


Fig 8. maximum force three-layers (First layer 4, second layer 17)

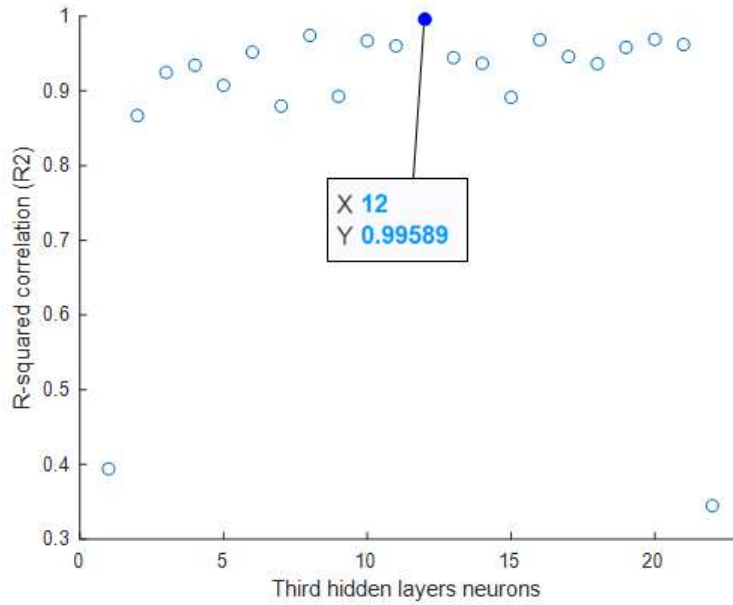


Fig 9. Fracture displacement three-layers (First layer 16, second layer 14)

According to Figs. 4 - 8, the best maximum force prediction is 0.99539 in one layer by seven neurons, 0.99947 in two layers by nineteen neurons at the first layer and six neurons at the second layer, as well as 0.999678 in three layers by four neurons at the first layer, seventeen neurons at the second layer, and three neurons at third layer. Moreover, the best fracture displacement prediction is 0.98087 by nineteen neurons, 0.99125 in two layers by nine neurons at the first layer and twelve neurons at the second layer, and 0.995895 in three layers by sixteen neurons at the first layer, fourteen neurons at the second layer, and twelve neurons a third layer. Fig 10 shows the results became better by increasing the hidden layer; however, the optimization time increased significantly. So, predicting the maximum force using a less hidden layer is logical, but fracture displacement prediction due to the complexity of its relations concerning GTN parameters, usage of a more hidden layer results better to reach suitable  $R^2$  net performance.

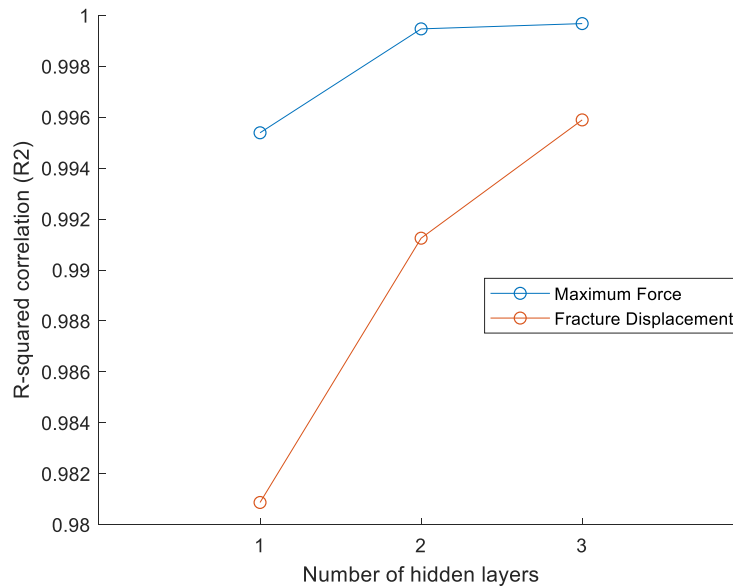


Fig 10. Effect of the number of layers on R<sup>2</sup> -value accuracy.

## Conclusions

In this work, the effect of the number of layers and neurons on the accuracy of ANN to predict of fracture behavior of Ti6Al4V alloys in the SLM process was investigated. Furthermore, the relation between the GTN fracture model coefficient, maximum force, and displacement was evaluated. The survey shows ANN is a proper method for obtaining the GTN fracture model coefficient and the number of hidden layers and training function in building a neural network as basic parameters of network classification have a large effect on the accuracy of the results, While the optimization time raises considerably. Therefore, concerning GTN parameters and the complexity of its results predicting the fracture displacement needs more hidden layers to achieve an accuracy of more than 99 %. The results demonstrate, due to more complexity of the relation for predicting fracture displacement higher layers achieve more accurate results, while for maximum force a less hidden layer results in acceptable accuracy as well as higher layers. It is suggested an ANN with higher layers and neurons can be employed for forecasting fracture displacement, while for maximum force, lower layers and neurons result in as same the higher one approximately.

## Disclosure statement

No potential conflict of interest was reported by the author(s).

## References

1. Safaei K, Abedi H, Nematollahi M, Kordizadeh F, Dabbaghi H, Bayati P, et al. Additive manufacturing of NiTi shape memory alloy for biomedical applications: review of the LPBF process ecosystem. *JOM*. 2021;1-16.
2. DebRoy T, Wei H, Zuback J, Mukherjee T, Elmer J, Milewski J, et al. Additive manufacturing of metallic components—process, structure and properties. *Progress in Materials Science*. 2018;92:112-224.
3. Majeed A, Ahmed A, Lv J, Peng T, Muzamil M. A state-of-the-art review on energy consumption and quality characteristics in metal additive manufacturing processes. *Journal of the Brazilian Society of Mechanical Sciences and Engineering*. 2020;42(5):1-25.
4. Patel A, Taufik M. Extrusion-Based Technology in Additive Manufacturing: A Comprehensive Review. *Arabian Journal for Science and Engineering*. 2022:1-34.
5. Lütjering G, Williams J. *Titanium, Engineering Materials and Processes*. Springer Berlin; 2007.
6. Elahinia M, Hashemi SM, Parvizi S, Baghbanijavid H, Tan AT, Nematollahi M, et al. Computational modeling of process-structure-property-performance relationships in metal additive manufacturing: a review. 2021.
7. Sahafnejad-Mohammadi I, Karamimoghadam M, Zolfagharian A, Akrami M, Bodaghi M. 4D printing technology in medical engineering: a narrative review. *Journal of the Brazilian Society of Mechanical Sciences and Engineering*. 2022;44(6):1-26.
8. Gholipour H, Biglari F, Nikbin K. Experimental and numerical investigation of ductile fracture using GTN damage model on in-situ tensile tests. *International Journal of Mechanical Sciences*. 2019;164:105170.
9. Hancock J, Mackenzie A. On the mechanisms of ductile failure in high-strength steels subjected to multi-axial stress-states. *Journal of the Mechanics and Physics of Solids*. 1976;24(2-3):147-60.
10. Rice JR, Tracey DM. On the ductile enlargement of voids in triaxial stress fields\*. *Journal of the Mechanics and Physics of Solids*. 1969;17(3):201-17.
11. McClintock FA. A criterion for ductile fracture by the growth of holes. 1968.
12. Gurson AL. Continuum theory of ductile rupture by void nucleation and growth: Part I—Yield criteria and flow rules for porous ductile media. 1977.
13. Tvergaard V, Needleman A. Analysis of the cup-cone fracture in a round tensile bar. *Acta metallurgica*. 1984;32(1):157-69.
14. Wilson-Heid AE, Furton ET, Beese AM. Contrasting the Role of Pores on the Stress State Dependent Fracture Behavior of Additively Manufactured Low and High Ductility Metals. *Materials*. 2021;14(13):3657.
15. Prieto A, Prieto B, Ortigosa EM, Ros E, Pelayo F, Ortega J, et al. Neural networks: An overview of early research, current frameworks and new challenges. *Neurocomputing*. 2016;214:242-68.
16. Nartu M, Dasari S, Sharma A, Mantri S, Sharma S, Pantawane MV, et al. Omega versus alpha precipitation mediated by process parameters in additively manufactured high strength Ti–1Al–8V–5Fe alloy and its impact on mechanical properties. *Materials Science and Engineering: A*. 2021;821:141627.
17. Tsai K-M, Luo H-J. An inverse model for injection molding of optical lens using artificial neural network coupled with genetic algorithm. *Journal of Intelligent Manufacturing*. 2017;28(2):473-87.
18. Wang F, Zhao J, Zhu N. Constitutive equations and an approach to predict the flow stress of Ti-6Al-4V alloy based on abt tests. *Journal of Materials Engineering and Performance*. 2016;25(11):4875-84.
19. Wang C, Tan X, Tor S, Lim C. Machine learning in additive manufacturing: State-of-the-art and perspectives. *Additive Manufacturing*. 2020;36:101538.
20. Chinchankar S, Shinde S, Gaikwad V, Shaikh A, Rondhe M, Naik M. ANN modelling of surface roughness of FDM parts considering the effect of hidden layers, neurons, and process parameters. *Advances in Materials and Processing Technologies*. 2022:1-11.

21. Mehrpouya M, Gisario A, Rahimzadeh A, Nematollahi M, Baghbaderani KS, Elahinia M. A prediction model for finding the optimal laser parameters in additive manufacturing of NiTi shape memory alloy. *The International Journal of Advanced Manufacturing Technology*. 2019;105(11):4691-9.
22. Mehrpouya M, Gisario A, Nematollahi M, Rahimzadeh A, Baghbaderani KS, Elahinia M. The prediction model for additively manufacturing of NiTiHf high-temperature shape memory alloy. *Materials today communications*. 2021;26:102022.
23. Kwon O, Kim HG, Ham MJ, Kim W, Kim G-H, Cho J-H, et al. A deep neural network for classification of melt-pool images in metal additive manufacturing. *Journal of Intelligent Manufacturing*. 2020;31(2):375-86.
24. Jimenez-Martinez M, Alfaro-Ponce M. Effects of synthetic data applied to artificial neural networks for fatigue life prediction in nodular cast iron. *Journal of the Brazilian Society of Mechanical Sciences and Engineering*. 2021;43(1):1-9.
25. Vafaenezhad H, Ghanei S, Seyedein S, Beygi H, Mazinani M. Process control strategies for dual-phase steel manufacturing using ANN and ANFIS. *Journal of materials engineering and performance*. 2014;23(11):3975-83.
26. Trivedi P, Vansjalia R, Erra S, Narayanan S, Nagaraju D. A Fuzzy CRITIC and Fuzzy WASPAS-Based Integrated Approach for Wire Arc Additive Manufacturing (WAAM) Technique Selection. *Arabian Journal for Science and Engineering*. 2022:1-20.
27. Popovich A, Sufiiarov V, Borisov E, Polozov IA, editors. *Microstructure and mechanical properties of Ti-6Al-4V manufactured by SLM*. Key Engineering Materials; 2015: Trans Tech Publ.
28. Needleman A, Tvergaard V. *Analyses of plastic flow localization in metals*. 1992.
29. Shafaie M, Khademi M, Sarparast M, Zhang H. Modified GTN parameters calibration in additive manufacturing of Ti-6Al-4 V alloy: a hybrid ANN-PSO approach. *The International Journal of Advanced Manufacturing Technology*. 2022:1-14.
30. Abaqus F. Dassault systemes simulia corporation. Providence, Rhode Island, USA. 2014.
31. MATLAB V. 9.6. 0.1072779 (R2019a). The MathWorks Inc: Natick, MA, USA. 2019.
32. Needleman A, Tvergaard V. An analysis of ductile rupture in notched bars. *Journal of the Mechanics and Physics of Solids*. 1984;32(6):461-90.
33. Tvergaard V. Material failure by void growth to coalescence. *Advances in applied Mechanics*. 1989;27:83-151.
34. Pujol J. The solution of nonlinear inverse problems and the Levenberg-Marquardt method. *Geophysics*. 2007;72(4):W1-W16.